Thermal and geochemical influences on microbial biogeography in the hydrothermal sediments of Guaymas Basin, Gulf of California

Luke McKay,[1,2,3]* Vincent W. Klokman,[1,4]
Howard P. Mendlovitz,[1] Douglas E. LaRowe,[5]
Daniel R. Hoer,[1] Daniel Albert,[1] Jan P. Amend[5,6] and
Andreas Teske[1]

[1]Department of Marine Sciences, University of North Carolina at Chapel Hill, Chapel Hill, NC 27599-3300, USA.
[2]Land Resources and Environmental Sciences, Montana State University, Bozeman, MT 59717, USA.
[3]Center for Biofilm Engineering, Montana State University, Bozeman, MT 59717, USA.
[4]Faculty of Health, Medicine and Life Sciences, Maastricht University, Maastricht, The Netherlands.
[5]Department of Earth Sciences, University of Southern California, Los Angeles, CA 90089, USA.
[6]Department of Biological Sciences, University of Southern California, Los Angeles, CA 90089, USA.

Summary

Extreme thermal gradients and compressed metabolic zones limit the depth range of microbial colonization in hydrothermally active sediments at Guaymas Basin. We investigated the physicochemical characteristics of this ecosystem and their influence on microbial community structure. Temperature-related trends of $\delta^{13}C$ values of methane and dissolved inorganic carbon from 36 sediment cores suggest *in situ* thermal limits for microbial anaerobic methane oxidation and organic carbon re-mineralization near 80°C and 100°C respectively. Temperature logging probes deposited in hydrothermal sediments for 8 days demonstrate substantial thermal fluctuations of up to 25°C. Putative anaerobic methanotroph (ANME) populations dominate the archaeal community, transitioning from ANME-1 archaea in warm surficial sediments towards ANME-1 Guaymas archaea as temperatures increase downcore. Since ANME archaea performing anaerobic oxidation of methane double on longer time scales (months) compared with relatively rapid *in situ* temperature fluctuations (hours to days), we conclude that ANME archaea possess a high tolerance for short-term shifts in the thermal regime.

Introduction

The Gulf of California is a relatively young ocean basin that is actively expanding as the North American and Pacific plates diverge via a system of narrow spreading zones interspersed by extended transform faults (Lizarralde *et al.*, 2007). The hydrothermal spreading centre of Guaymas Basin, located in the central Gulf of California at a water depth of 2000 m, is buried by up to 400 m of organic-rich sediments. Fresh magmatic sills intrude into the thick sediment layer squeezing hot, chemically altered fluids through fissures upward to the seafloor (Einsele *et al.*, 1980). Thermocatalytic transformation of buried organic matter results in a hydrocarbon-rich sedimentary environment (Bazylinski *et al.*, 1988; Didyk and Simoneit, 1989). Cold, oxygenated bottom water mixes with buoyantly rising hydrothermal fluids, creating steep physicochemical gradients in the surficial sediments (Gundersen *et al.*, 1992). The shallow subsurface microbial community at Guaymas Basin takes advantage of a variety of substrates and thermal conditions, and diverse microbial processes characterize the upper sediments, including microbial sulfate reduction, sulfide oxidation, methanogenesis and the anaerobic oxidation of methane (AOM) (Teske *et al.*, 2014).

Anaerobic oxidation of methane was first implicated in Guaymas Basin by the presence of 16S ribosomal (r)RNA genes and ^{13}C-depleted archaeal lipids of anaerobic methanotrophic (ANME) archaea (Teske *et al.*, 2002; Schouten *et al.*, 2003), and has since become recognized as a dominant microbial process in these sediments. *Ex situ* AOM rates were determined in high temperature and high-pressure laboratory incubations (Kallmeyer and Boetius, 2004). More recently, specialized thermophilic or at least thermotolerant ANME *Archaea* were found at Guaymas Basin (Holler *et al.*, 2011; Biddle *et al.*, 2012). Methane, hydrocarbons and low-molecular weight organic acids, produced from pyrolysis of buried organic matter, provide substrates for sulfate reduction, a microbial

re-mineralization process that is supported by several lines of evidence in Guaymas Basin sediments: the frequent recovery of deltaproteobacterial 16S rRNA or dissimilatory sulfite reductase genes (Teske *et al.*, 2002; Dhillon *et al.*, 2003; Holler *et al.*, 2011; Biddle *et al.*, 2012); sulfate reduction rate measurements at mesophilic, thermophilic and hyperthermophilic temperature regimes (Jørgensen *et al.*, 1990; 1992; Elsgaard *et al.*, 1994; Weber and Jørgensen, 2002; Meyer *et al.*, 2013); and the strong sulfide accumulation observed in hydrothermally affected cores (Jørgensen *et al.*, 1990; Weber and Jørgensen, 2002; Biddle *et al.*, 2012).

Here, we explore how geochemical signatures of methane oxidation and organic matter re-mineralization at multiple sediment sites in Guaymas Basin indicate the *in situ* thermal limits of these microbial processes. We selected a hydrothermally active sediment site for integrated geochemical, thermal, molecular and thermodynamic characterization, with special attention to biogeographical structuring of ANME subgroups. With continuous temperature logging of this hydrothermal hot spot for 8 days, we document the dynamic conditions that shape local microbial community structure and habitat preference.

Results and discussion

Sampling site selection

Using *Beggiatoa* mats as a visual indicator of hydrothermal flow (McKay *et al.*, 2012), *in situ* temperature profiles and matching push cores were collected from a wide range of mats; non-hydrothermal sediments were included as controls (data reported in Table S1). A well-developed orange and white *Beggiatoa* mat was chosen for a core transect based on the *a priori* concept that the transition from bare sediment to white and then to orange *Beggiatoa* mats indicates an intensifying hydrothermal gradient in the underlying sediment (McKay *et al.*, 2012). A core from a different white *Beggiatoa* mat with a similar thermal profile to the core from the white section of the transect mat was selected for comparison of subsurface geochemistry and microbial diversity.

Comparisons of temperature and porewater geochemistry

Most surface layer sediments (0–3 cmbsf) retain bottom water temperatures of approximately 3°C, while at a sediment depth of just 40 cmbsf temperatures range from 3°C in hydrothermally inactive sediments to 200°C in sediments with extreme hydrothermal activity ($n = 130$; McKay *et al.*, 2012). Site-specific variation in hydrothermal activity is accompanied by varied levels of pyrolysed and

hydrothermally altered organic material, and variable delivery of hydrothermally derived electron donors and carbon sources; for example, pore water concentrations range from 0 to 28.3 mM methane (average 2.56 mM) and from 1.58 to 68.4 mM dissolved inorganic carbon (DIC), with an average of 16.0 mM (Fig. 1A, B). To investigate possible correlations between hydrothermal activity and substrate availability, we compared *ex situ* pore water methane and DIC concentrations with corresponding temperatures from 36 sediment cores sampled in 2008 and 2009 (Fig. 1A, B). The methane and DIC concentrations do not correlate well with thermal conditions; increasing methane concentration and increasing temperature, and decreasing DIC concentration and increasing temperature show no significant correlation ($r^2 = 0.06$ and $r^2 = 0.02$ respectively). The surficial sediments examined here are replete with methane and DIC over a wide temperature range, so much that the pore water concentrations of these compounds do not allow the identification of specific abiotic or microbial sources. Therefore, we examine stable isotopic signatures for pore water methane and DIC as potential indicators for biogenic sources and microbial processing of these compounds.

Thermal range of anaerobic methane oxidation

To investigate the thermal range of two microbial processes – anaerobic methane oxidation and heterotrophic organic carbon re-mineralization – we compared stable isotopic values for methane and DIC with their corresponding temperatures at specific sediment horizons, and examined them for a possible biogenic imprint (Fig. 1). The $\delta^{13}C$ signatures of methane at most marine hydrothermal systems indicate a predominantly abiotic origin; examples include −15‰ at 21°N East Pacific Rise (Welhan and Craig, 1983), between −14‰ and −7‰ at the Lost City serpentinite hydrothermal system (Kelley *et al.*, 2005), and −16‰ for plume fluids ejecting from the Myojin Knoll Caldera (Tsunogai *et al.*, 2000). By contrast, the hydrothermal methane at Guaymas Basin originates from pyrolysis of buried photosynthetic organic matter at high temperatures, and produces a higher degree of ^{13}C-depletion, with a reported $\delta^{13}C$ range between −43‰ and −51‰ (Welhan and Lupton, 1987; Welhan, 1988). Our measured $\delta^{13}C$ values for pore water methane from multiple sites of variable hydrothermal activity range from −74.2 ‰ to −6.4 ‰ with an average value of −37.9 ‰.

The laboratory temperature maximum for microbial growth is 122°C (Takai *et al.*, 2008), and *in situ* microbial activity in the sedimentary subsurface, for example microbial petroleum degradation, has an upper limit of *c.* 80°C (Head *et al.*, 2003). Therefore, the $\delta^{13}C$-CH$_4$ values of samples with *in situ* temperatures above 150°C – in this data set, −39.1‰ to −43.2 ‰ – should preclude microbial
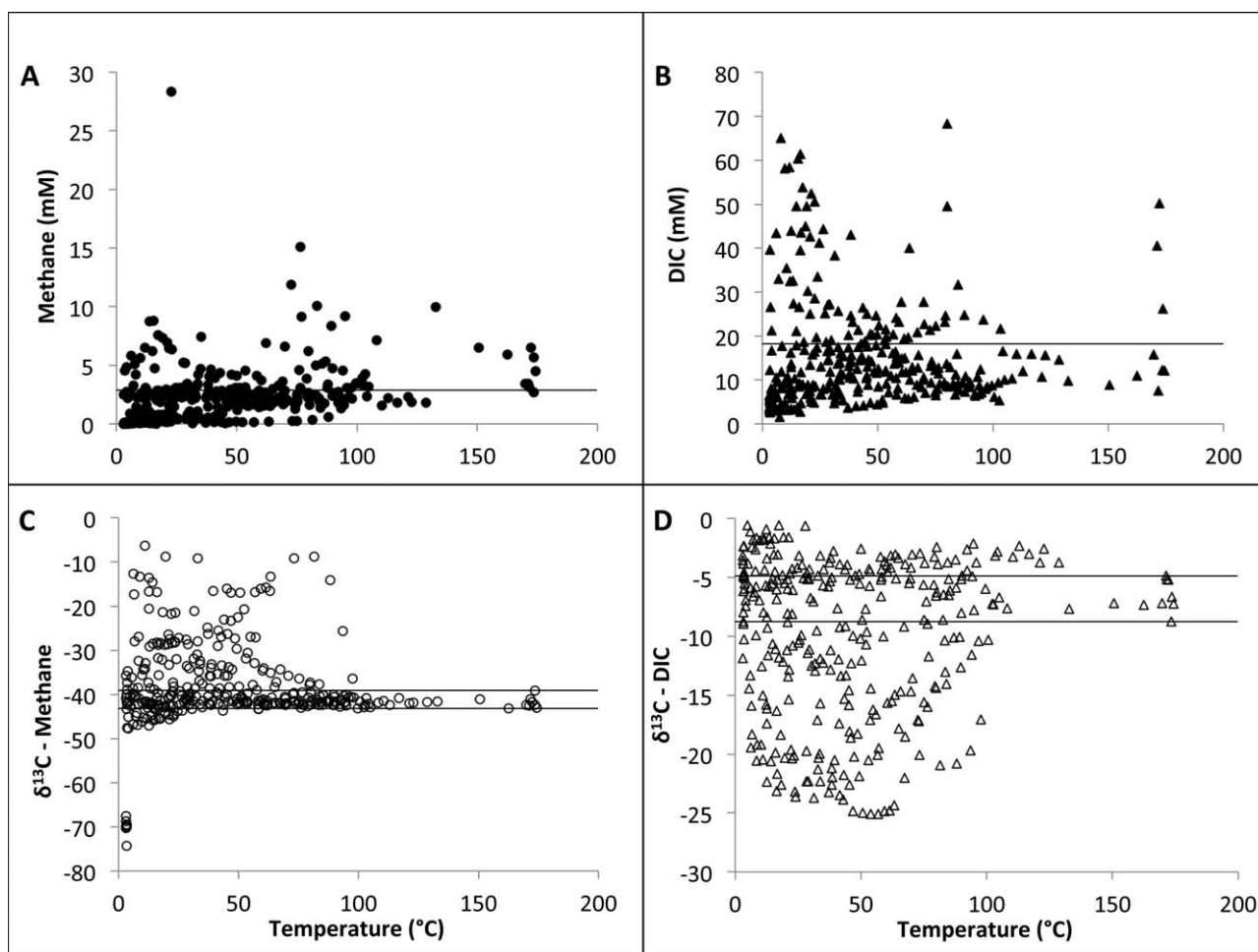
Fig. 1. Pore water concentrations and δ¹³C-signatures versus *in situ* temperature for methane concentrations (A), DIC concentrations (B), δ¹³C-methane values (C) and δ¹³C-DIC values (D). For methane and DIC average concentrations are represented by solid lines (A and B). For stable isotope plots of methane (C) and DIC (D), black lines indicate the maximum and minimum δ¹³C isotopic values at temperatures above 150°C. For alternate plots of the same data, see Fig. S4.

alteration by a wide temperature margin. This range of δ¹³C-CH₄ (solid lines, Fig. 1C) is consistent with previous δ¹³C-CH₄ measurements from Guaymas Basin hydrothermal fluids above 300°C, for which three out of four measurements were near −43‰ (Welhan and Lupton, 1987; Pearson *et al.*, 2005). The consistency of this baseline is remarkable and suggests sustained pyrolytic methane production, possibly in combination with a shared methane subsurface reservoir, at all coring sites in the southern Guaymas spreading centre (all within a few hundred meters; Meyer *et al.*, 2013). Microbial methane oxidation would enrich the residual methane pool in ¹³C-CH₄ as compared with the source methane, and result in values > −39.1‰. With the exception of a single sediment core, all 36 cores sampled in 2008 and 2009 indicate that ¹³C-enriched methane (δ¹³C-CH₄>−39.1‰,) is not detected above 75–80°C (Fig. 1C); we therefore conclude that this temperature is a strong candidate for the *in situ*

thermal limit of microbial AOM in Guaymas sediments. This inferred thermal limit is consistent with previous *ex situ* enrichments of Guaymas sediments which indicated that AOM could not be detected at temperatures ≥ 75°C (Holler *et al.*, 2011).

This argumentation implies that methane with a specific, biologically interpreted isotopic signature originates from the same location and sediment horizon where it has been measured, and is therefore representative for a biological imprint at the *in situ* temperature regime; yet lateral and vertical advective transport and mixing in hydrothermally active sediments (Gundersen *et al.*, 1992) could stretch and sever this link. In this case, δ¹³C-CH₄ values plotted against temperature should produce a randomized pattern without any specific temperature dependent relationship. Individual geochemical profiles indicate considerable site-to-site δ¹³C-CH₄ variability at temperatures below 80°C, probably resulting from advective influences. When

compiling all available data, the apparent 80°C *in situ* temperature limit for ^{13}C-CH_4 enrichment remains intact. This observation indicates that a biological factor – anaerobic methane oxidation – counteracts overprinting of the $\delta^{13}C$-CH_4 signature by advective transport and mixing.

As a potential caveat, microbial methane oxidation may exist at temperatures higher than 80°C, but could be isotopically invisible due to overabundant hydrothermal methane. If so, the isotopic imprint of hyperthermophilic AOM should reveal itself at lower methane concentrations. Yet, for all samples below the methane concentration limit where AOM could be detected (4.36 mM), a majority (88%, $n = 43$) of high temperature samples (>80°C) are clustered within the −43‰ to −39‰ range. In other words, isotopic values for methane in high temperature sediments remained within the hydrothermal baseline of Guaymas Basin, even when samples with low methane concentration were considered, where AOM imprint should be easily visible. The simplest explanation for this observation is the thermal limitation of microbial AOM at temperatures that exceed 80°C.

Finally, the possibility has to be considered that biotic isotopic fractionation of AOM could decrease at extremely high temperatures and *in situ* pressure, analogous to results for methane production by a hyperthermophilic methanogen, *Methanopyrus kandleri* (Takai *et al.*, 2008). Without additional pure culture or enrichment experiments, this possibility cannot be ruled out, but at present there is no evidence to support such a possibility.

Thermal range of organic matter re-mineralization

The compiled $\delta^{13}C$-DIC values suggest thermal constraints on the microbial process of organic matter re-mineralization (OMR). In Guaymas Basin, the $\delta^{13}C$-DIC values prior to sedimentary microbial processing range from −0.6‰ in bottom water (Pearson *et al.*, 2005) to −9.4‰ in hydrothermal fluids (Seewald *et al.*, 1998) (dashed lines, Fig. 1B). Our sediment porewater $\delta^{13}C$-DIC values range from −25.1‰ (within the range of biomarkers of buried marine algae, −21‰ to −28‰, Teske *et al.*, 2002) to the bottom water value of −0.6‰. Almost all (96%) $\delta^{13}C$-DIC values from sediments with *in situ* temperatures greater than 100°C ($n = 23$) are less ^{13}C-depleted than −8.8 ‰, the lightest $\delta^{13}C$-DIC value associated with abiotic sediments above 150°C (Fig. 1D). More strongly ^{13}C-depleted DIC values, below −9.4‰, likely indicate the influence of microbially mediated OMR, and are primarily associated with temperatures below 100°C. While several low temperature $\delta^{13}C$-DIC values occur within the abiotic range – indicating other variables controlling OMR favourability – only one high temperature $\delta^{13}C$-DIC value is more ^{13}C-depleted than the abiotic

range. These observations strongly suggest that microbial re-mineralization of organic carbon is thermally restricted to temperatures below 100°C. This inferred *in situ* temperature limit for OMR has to be qualified by the same caveats as those discussed for AOM.

Specific sites in Guaymas Basin

In addition to examining the complete data set of stable carbon isotopic signatures to infer *in situ* temperature limits on AOM and OMR, we selected five specific sites for long-term temperature monitoring and additional molecular and geochemical analyses that cannot be applied to all sampling locations. Namely, we investigated a transect of three cores from the centre to the margin of a mat-covered microbial hot spot (the orange central mat, the white mat periphery and the bare sediment surrounding the hot spot), another hydrothermal hot spot covered with a white mat (with a similar thermal profile to the previous white mat periphery sediments) and bare sediment with no hydrothermal activity. These sites were examined by geochemical profiling of the pore water DIC, methane, sulfate and sulfide (Fig. 2), by multi-day temperature logging of the hydrothermal gradients (Fig. 3), by thermodynamic modelling of AOM energy yield based on these pore water profiles (Fig. 4), and by 16S rRNA analysis of the bacterial and archaeal communities (Fig. 5), further extended with PCA of the different microbial communities in their distinct thermal habitats (Fig. S1). These combined analyses were used to further develop our hypotheses concerning the thermal range of microbial processes in hydrothermal sediments of Guaymas Basin.

Porewater geochemical profiles

The five cores were characterized by downcore profiles of temperature, methane concentrations and stable carbon isotope values, DIC concentrations and stable carbon isotope values and sulfate and sulfide concentrations (Fig. 2). The high CH_4, DIC and sulfide concentrations for the orange and white mat cores (4569-9, 4569-2 and 4571-4) indicating strongly reducing hydrothermally influenced conditions, contrasted with lower concentrations in bare sediment core 4569-4 and control core 4567-28. The $\delta^{13}C$-CH_4 profiles show the pervasive imprint of methane oxidation in heavy isotopic values around −30‰ to −15‰, occurring in surficial layers in the hottest orange mat core, and in deeper layers in the other cores; no $\delta^{13}C$-CH_4 data exist for the background core. The $\delta^{13}C$-DIC profiles show relatively heavy DIC, in the range of −5‰, in the surface layers of the cool cores where seawater influence is likely; the lightest values in the range of −25 to 30‰ are found at depth in the white mat cores (4569-2 and 4571-4), indicating DIC contributions from organic matter
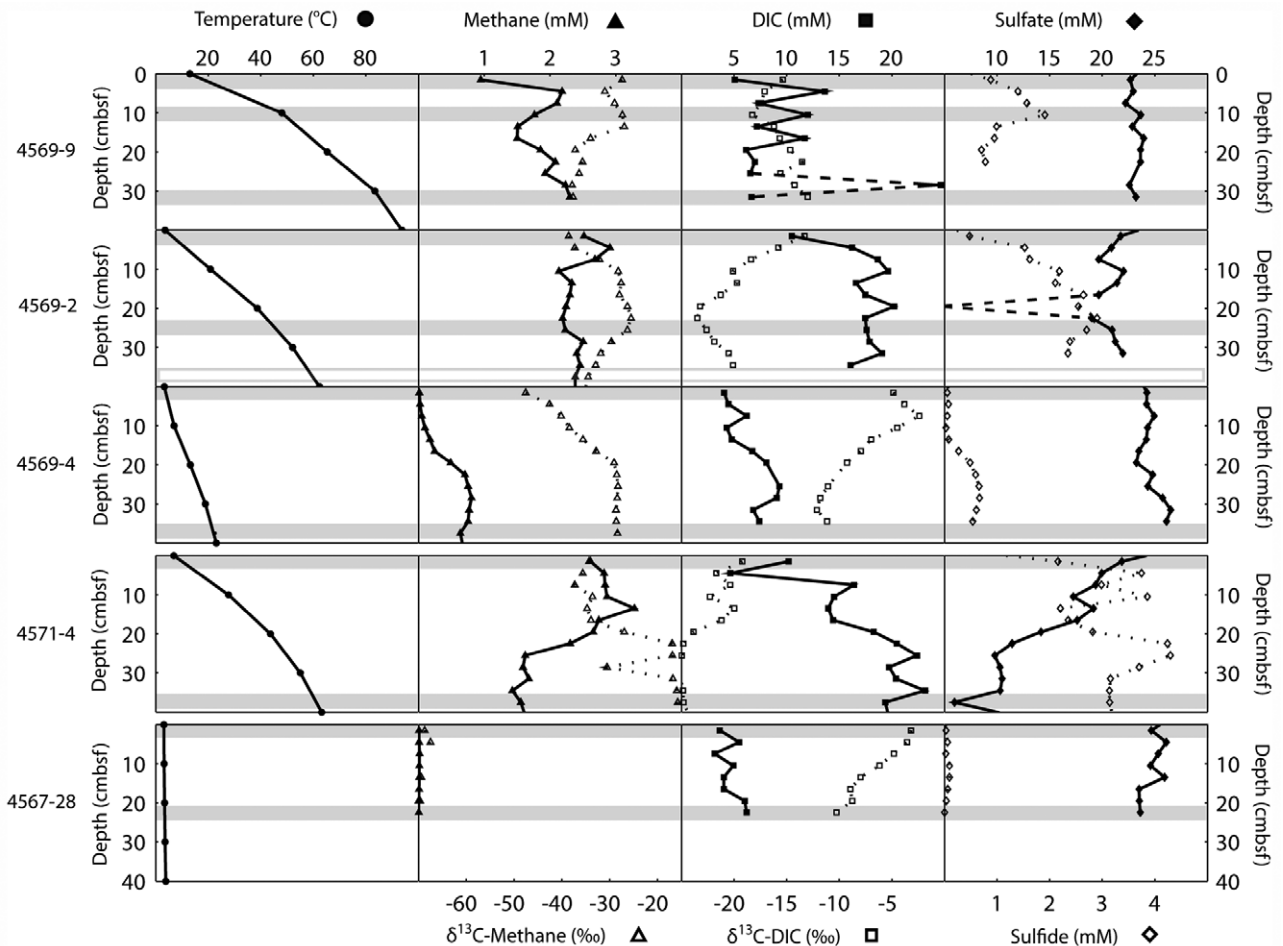
Fig. 2. Temperature and geochemical profiles for five individual cores. Shallow 40 cm subsurface profiles for *Alvin* heat flow probe temperature, pore water methane concentrations and δ¹³C isotopic signatures, DIC concentrations and δ¹³C isotopic signatures, and sulfate and sulfide concentrations are plotted for three cores in a transect across a *Beggiatoa* mat (4569-9, 4569-2 and 4569-4), a core from a different *Beggiatoa* mat (4571-4) and a background core with no hydrothermal activity (4567-28). The data for cores 4569-9, 4569-2 and 4569-4 were previously published (McKay *et al.*, 2012). Filled in shapes correspond to the top axes and open shapes correspond to the bottom axes. Grey bands indicate sampling depths for archaeal and bacterial clone libraries.

re-mineralization and methane oxidation. Interestingly, only core 4571 is showing downcore sulfate depletion; the other hydrothermal cores remain well supplied with sulfate, a possible consequence of hydrothermal mixing of surface water into the sediments. Detailed core-by-core descriptions of the pore water profiles are included in Supplementary online materials.

Temperature fluctuations in shallow sediments

At four of the five individual coring sites examined in this study, temperature logging probes were deployed for 7 to 8 days prior to coring. Three temperature logging probes were placed in a transect across a well-developed *Beggiatoa* mat from the central orange region to the white mat periphery to the bare sediments adjacent to the mat (McKay *et al.*, 2012); a fourth temperature logging probe

was inserted in the white section of a different *Beggiatoa* mat a few meters away. The temperature logging probes are named for the sediment cores taken next to them: 4569-9 in the orange section, 4569–2 in the white mat, 4569-4 adjacent to the mat and 4571-4 in the white section of the other mat (Fig. 3). The three coring sites show consistently cold sediment–water interface temperatures (on average 5°C at 4569-9, 3°C at 4569-2 and 4569-4) but distinctly variable subsurface temperatures over time and downcore. The central mat core 4569-9 is characterized by widely fluctuating temperatures in the upper sediment layers (*c.* 40 to 60°C at 10 cm depth) that are changing on the scale of hours, and steadier high temperatures (85–90°C) in the deepest sediments. The temperatures next to the white mat core 4569-2 are steadily increasing at all depths throughout the first 4 days, before stabilizing for the remainder of the logging period and reaching 75°C in the
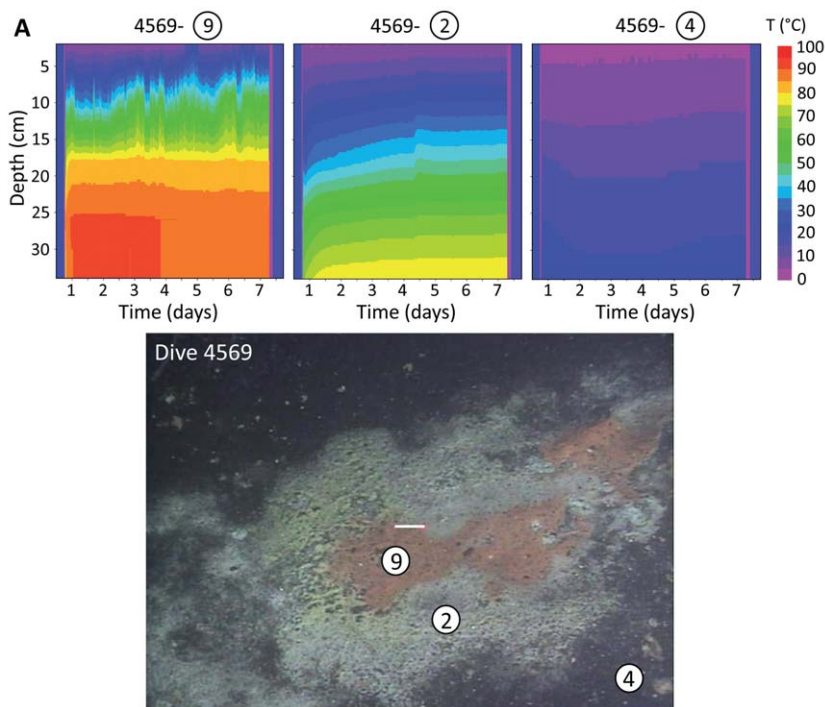
Fig. 3. Temperature logging probe measurements. Temperatures were measured over a 7–8 day period at four distinct sediment sites. Temperatures were recorded at five discrete depths and linearly interpolated at a resolution of 20 discrete colours. White bars in the photographs represent a distance of 10 cm.
A. Three temperature logging probes were deployed in transect across a *Beggiatoa* mat. The numbers at the logging locations in the orange and white mat (9 and 2) and the bare sediment (4) match the push core numbers collected during Alvin Dive 4569 adjacent to these locations at the conclusion of the temperature logging survey.
B. One probe was inserted into the white portion of another *Beggiatoa* mat (appearing grey on this photo due to sediment suspension and re-deposition during sampling) a few meters away from the mat displayed in section A of this figure. The T-logger sank 3 cm between days 6 and 7, resulting in the temperature shift observed.
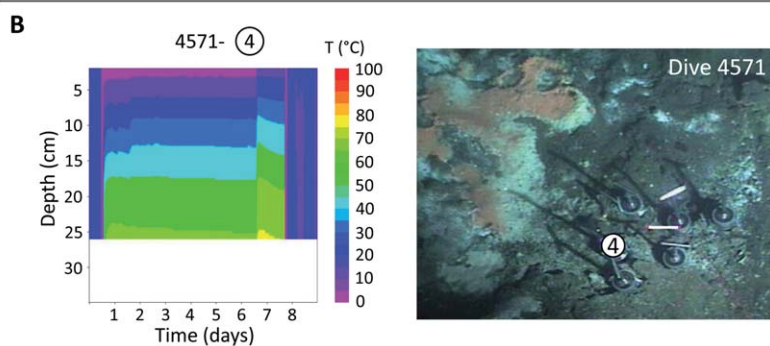
deepest sediments. Bare sediment core 4569-4 is characterized by a moderate temperature gradient (max. 24°C at depth) that remains constant over time. The temperature logging results for white mat core 4571-4 are similar in range to those of white mat core 4569-2, increasing from 3°C at the surface to approximately 75°C at depth. Short-term thermal fluctuations on the scale of hours were superimposed on longer term temperature increases and decreases appearing on the scale of several days. The white mat sediments next to core 4569-2 showed a gradual temperature increase over the T-logging period, whereas the nearby orange mat sediments (core 4569-9) showed a slight temperature decrease at depth and – in part overprinted by fluctuations – a slight temperature increase in the surficial layers. The sharp temperature increase occurring on day six of the T logger deployment was caused by the probe sinking a few cm further into the soft mud, documented by *Alvin* frame-grabber images immediately after probe deployment and before recovery.

These time-resolved temperature gradients show that the thermal limits of microbial processes, such as AOM and OMR, should be understood not only as absolute limits but within the context of thermal variation over time. Thermal variability over hours or days will impact the resident microbial community, which must tolerate these short and long-term shifts in the *in situ* thermal regime in addition to coping with high temperatures associated with hydrothermally active sediments. Given the frequency of temperature shifts on a scale of hours to days, the remarkably low doubling time of microorganisms performing AOM at 68 days (Holler *et al.*, 2011), and the predominance of ANME-related 16S rRNA gene sequences recovered from Guaymas sediments (this study; Biddle *et al.*, 2012; Teske *et al.*, 2002), it stands to reason that ANME *Archaea* should have a high tolerance for shifts in *in situ* temperature. If frequent jumps in temperature were to wipe out the ANME community, they would not have enough time to re-colonize the sediments before the next
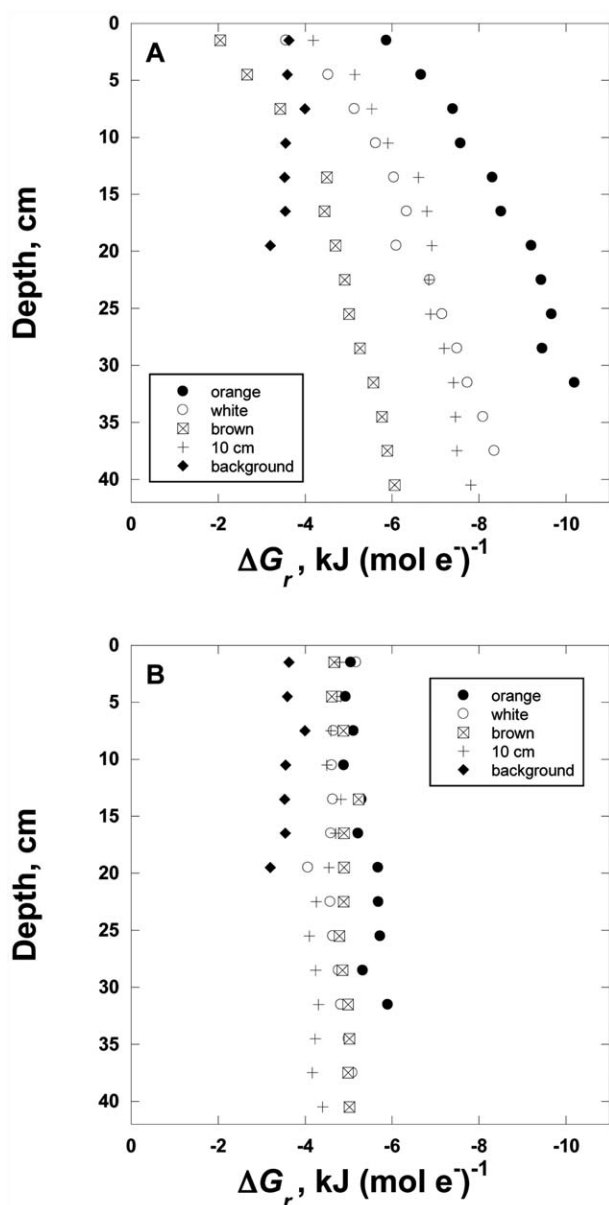
Fig. 4. Gibbs energy, ΔG_r, of AOM with sulfate in five individual cores.
A. Calculations are based on dynamic pH values extrapolated from measured temperature-pH curves at distinct Guaymas sites to the samples from this study. At higher temperatures, pH becomes very low (c. 2), thereby increasing the favourability of the reaction.
B. Calculations are based on a fixed pH value of 5.9 taken from the literature (Von Damm *et al.*, 1985). See supplementary text for additional details.

major temperature shift occurred. This conclusion underscores the importance of considering adaptations to dynamic environmental conditions, particularly in extreme ecosystems. Microorganisms that are able to survive short-term temperature spikes may succumb to sustained hydrothermal peaks; heat-sterilized sediments would then be re-occupied by fast-growing microbial colonizers that

may even depend on hydrothermal disturbance. It is possible that in some sediments, hydrothermal disturbance rarely permits the establishment of a stable microbial community.

Energy yield of high-temperature AOM

Temperature measurements, pore water concentrations of methane, DIC, sulfate and sulfide (Fig. 2), salinity (M. Zabel, unpubl. data), and pH (D. de Beer ,unpubl.data) were used to model the Gibbs energy yield of AOM in the hydrothermal sediments of the five model cores (Fig. 4). Calculations of ΔG_r of the suggested reaction for sulfate-dependent AOM had previously shown that this process remains exergonic at elevated temperatures (LaRowe *et al.*, 2008), but can be prohibited due to low CH_4 and sulfate concentrations at high temperatures (LaRowe *et al.*, 2014). The Gibbs energy of this reaction is strongly dependent on the *in situ* methane concentrations and temperature, but also on pH, which was not measured *in situ*. Two scenarios were therefore considered: (i) low-pH conditions extrapolated from temperature-correlated pH gradients determined by *in situ* microelectrode measurements in different Guaymas Basin mat-covered sediments (D. de Beer, pers. comm.); and (ii) an *ex situ* pH of 5.9, previously published for Guaymas Basin hydrothermal fluids (Von Damm *et al.*, 1985). Compared with the low-pH regime, the moderate pH conditions reduce the favourability of sulfate dependent AOM, but higher temperatures increase the favourability of the reaction in both cases (Fig. 4A, B). Regardless of which pH model is used in the calculations, sulfate-dependent AOM is consistently exergonic ($\Delta G_r < 0$). The recently suggested reaction mechanism linking AOM to sulfur disproportionation (Milucka *et al.*, 2012) would alter the profiles, which represent AOM coupled directly to sulfate reduction. However, because both processes are stoichiometrically equivalent, AOM coupled to sulfur disproportionation retains the same general trend of increasing favourability with depth and temperature.

The existing temperature limits of AOM are therefore not a consequence of limiting energy yield but most likely result from thermal sensitivity of cellular compounds and enzymes and increased maintenance energy. The benefit of increased thermodynamic potential for sulfate-dependent AOM in deeper, hotter and more acidic sediments is likely overshadowed by the increase in maintenance energy requirements under harsher conditions. While an increase in temperature by 20°C increases the Gibbs energy yield by approximately 10 kJ mol^{-1} CH_4 (Fig. 4A; 8 e$^-$ transferred per mole CH_4 oxidized), this same change in temperature increases the power requirement of maintenance energy by an order of magnitude (Tijhuis *et al.*, 1993). The shifting balance between AOM energy
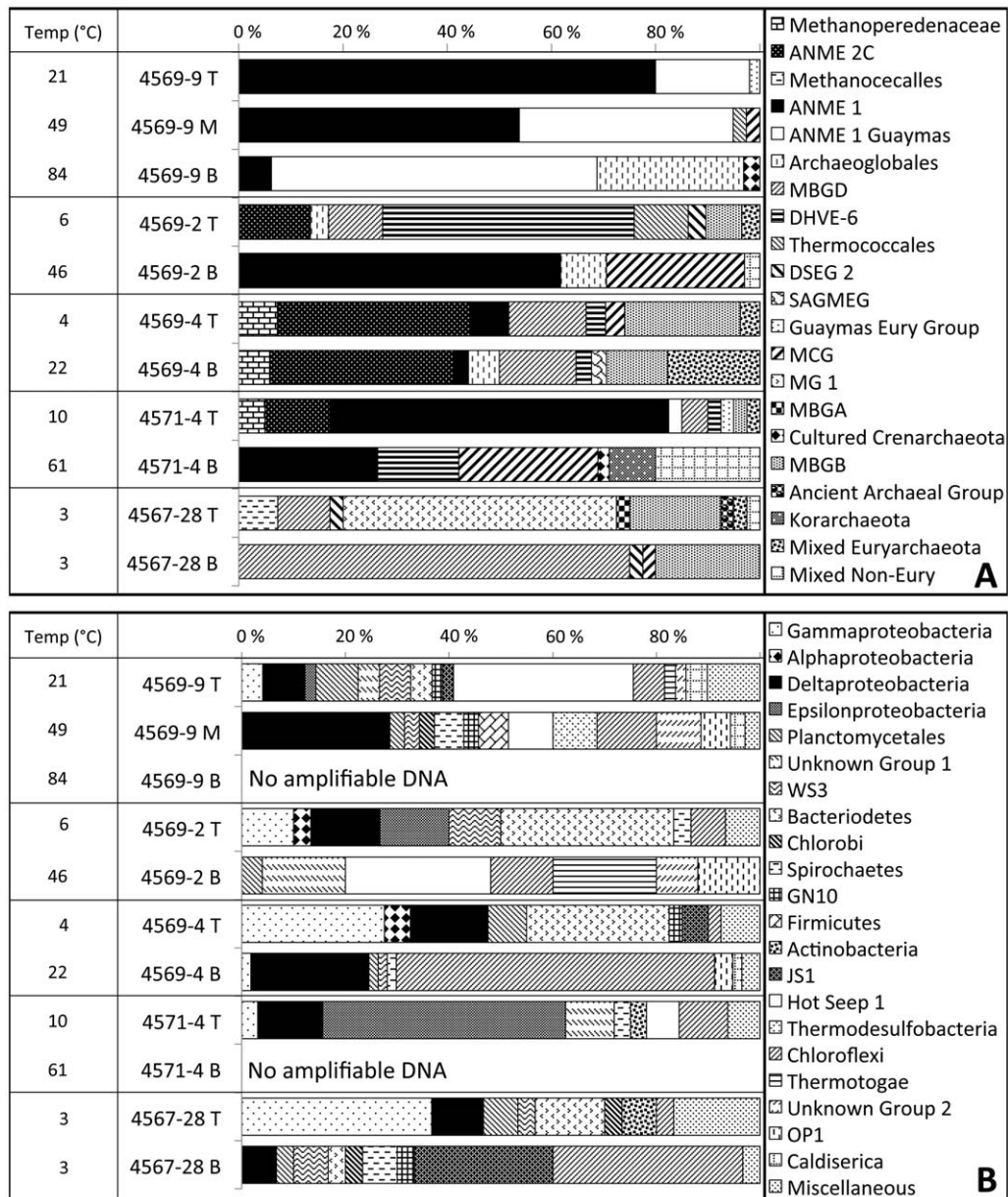
Fig. 5. Clone distribution bar graphs for 16S rRNA gene libraries. Relative distributions of clone recovery are presented at the phylum-to-class level for the five cores studied for *Archaea* (A) and *Bacteria* (B). Each bar represents a sampled section of one of the five cores which are indicated further by the grey shaded areas in Fig. 3. Three sections were sampled for the hottest core in the microbial mat transect (4569-9) while only two sections, the top and the bottom, were sampled from the other cores. *In situ* temperatures for each section are listed on the far left. Sequence recovery for each sample is here reported first for *Archaea* and then for *Bacteria*: 4569-9 T (50, 49), 4569-9 M (39, 35), 4569-9 B (32, 0), 4569-2 T (29, 30), 4569-2 B (34, 25), 4569-4 T (27, 40), 4569-4 B (34, 57), 4571-4 T (40, 32), 4571-4 B (45, 0), 4567-28 T (40, 30) and 4567-28 B (40, 30).

yield and maintenance energy of thermally stressed cells is likely to limit the temperature range of AOM.

16S rRNA gene profiles

The microbial community structure of the five cores discussed above was analysed by 16S rRNA gene cloning and sequencing, using extracted DNA from the top and bottom of each core, and an additional mid-section sample for the hottest core, 4569-9. Phylogenetic relationships of total 16S rRNA gene clones recovered from these core sections are reported in neighbour-joining trees separately for *Archaea* and *Bacteria* (Fig. S2A,B). The Guaymas clones were assigned to monophyletic groups – 21 within the *Archaea* and 20 within the *Bacteria* – that were identified based on previously recovered operational taxonomic

units (OTUs) and cultured isolates. The composition of the archaeal and bacterial clone libraries distribution is plotted for each location and depth layer in bar diagrams (Fig. 5A, B). The nine groups with the highest number of representatives in the archaeal clone library, in order from highest to lowest, are ANME-1 (Hinrichs *et al.*, 1999), Marine Benthic Group D (MBG-D, Vetriani *et al.*, 1999), ANME-1 Guaymas (Biddle *et al.*, 2012), ANME-2c (Orphan *et al.*, 2001), Marine Benthic Group B (MBG-B, Vetriani *et al.*, 1999), Miscellaneous Crenarchaeotal Group (Inagaki *et al.*, 2003), Deep-sea Hydrothermal Vent Euryarchaeota Group 6 (Takai and Horikoshi, 1999), Marine Group 1 (MG-1, DeLong, 1992) and *Archaeoglobales*. Together, the ANME archaeal lineages ANME-1, ANME-1 Guaymas, ANME- 2c and *Methanoperedenaceae* (Fig. 5A; Fig, S2A) account for 51% of the total archaeal 16S rRNA gene recovery (208 out of 410 clones), and emphasize the role of anaerobic methane oxidation in the Guaymas hydrothermal sediments.

The archaeal clone library results indicate that temperature and redox regimes define the habitats and *in situ* occurrence patterns of most of these groups (see detailed discussion in SOM). Although AOM remains feasible over a wide temperature range, the methane-oxidizing community changes with depth. Anaerobic methanotroph *Archaea*-related sequences represent the largest fraction (63%) of the archaeal 16S rRNA gene clones recovered from the four hydrothermally active cores ($n = 330$). All ANME OTUs were related to *Archaea* belonging to the ANME-1, ANME-2c and the family-level candidatus taxon *Methanoperedenaceae* (Fig. 5A; Fig. S2A). The background core, with negligible methane concentrations (≤ 0.01 mM), did not yield any ANME phylotypes. Anaerobic methanotroph 2c archaea are prevalent in Guaymas sediments but also appear to be thermally and/or geochemically restricted; 16S rRNA gene recovery demonstrates ANME-2c presence only in the cool core (4569-4) and the cool surface layers of the two warm cores (4569-2, 4571-4). Anaerobic methanotroph 1 archaeal phylotypes were present in the cool, warm and hot cores in both the surface and deep sediment layers. Investigation of the ANME-1 group at higher resolution permits parsing out thermally structured subgroups. The ANME-1 Guaymas group, a separate ANME-1 lineage that is distinct from the widely distributed ANME-1a Guaymas and ANME-1b groups (Biddle *et al.*, 2012; Merkel *et al.*, 2013), appears to be enriched in clone libraries as temperatures increase in the hottest core (4569-9), dominating clone library recovery in the deepest layer at 84°C. Anaerobic methanotroph 1 Guaymas *Archaea* are a group of putatively thermophilic anaerobic methane oxidizers that are consistently recovered from hot Guaymas sediments (Teske *et al.*, 2002; Biddle *et al.*, 2012; Merkel *et al.*, 2013). We hypothesize that the ANME-1 Guaymas group represents thermophiles

that can access the methane pool near the AOM temperature maximum. All other ANME-1 *Archaea* account for reduced fractions of the archaeal clone libraries with increasing temperatures. The clone library results suggest that ANME-2c archaea are associated with cooler or surficial, potentially more oxidized sediments (<20°C), while most ANME-1 archaea tolerate warmer sediments, consistent with *ex situ* enrichment at 37°C (Kellermann *et al.*, 2012) and 50°C respectively (Holler *et al.*, 2011).

Considering 80°C as our inferred upper thermal limit for AOM, these occurrence patterns indicate that ANME-1 archaea and ANME-1 Guaymas archaea persist throughout the thermal range of AOM, with ANME-1 Guaymas archaea prevailing towards high temperatures in deeper sediment layers. To the best of our knowledge, this is the first case study demonstrating ANME-1/ANME-1 Guaymas transitions within the same sediment core and mat field. As a caveat, these cores did not reach into deeper, permanently hot sediment layers with temperature regimes above 80°C; therefore we do not have sequence-based evidence of the temperatures where ANME sequence signatures will ultimately disappear. This data set is limited to showing survival and presence of ANME lineages over a thermal range that includes 80°C. We also note that temperature is not the only factor controlling ANME distribution; the redox state also plays an important role (Biddle *et al.*, 2012), and other unconstrained variables such as pH cannot be ruled out.

Bacterial 16S rRNA gene clones were recovered from all samples except those at the two hottest depths (4569-9B and 4571-4B). The bacterial clone libraries were dominated by members of the *Chloroflexi*, *Deltaproteobacteria*, the HotSeep-1 group (Holler *et al.*, 2011), *Gammaproteobacteria*, *Bacteriodetes*, *Epsilonproteobacteria*, *Planctomycetales* and the uncultured lineages Japan Sea Group 1 (Webster *et al.*, 2004) and WS3 (Dojka *et al.*, 1998). After the highly abundant *Chloroflexi*, a phylum that is widespread in marine sediments, the second most abundant bacterial group were the *Deltaproteobacteria*, harbouring numerous genera of sulfate-reducing bacteria (Muyzer and Stams, 2008) and ANME syntrophs that are prevalent in marine sediments (Knittel and Boetius, 2009) (see SOM for details on other *Deltaproteobacteria*-related groups). Members of the HotSeep-1 group constituted the third-most frequently recovered lineage and accounted for 24% of the total 16S rRNA gene recovery within the bacterial clone library (Fig. 5B; Fig. S2B). In contrast to previous usage (Holler *et al.*, 2011), we separate the HotSeep-1 group from the *Deltaproteobacteria*, since multi-phylum phylogenetic analyses identified the HotSeep-1 group and the *Hippea-Desulfurella* cluster as separately branching lineages that cannot be included in the *Deltaproteobacteria*

(Fig. S3). Members of the HotSeep-1 group were first enriched at 60°C in butane-amended samples from Guaymas Basin (Kniemeyer *et al.*, 2007); they are of special interest in the context of anaerobic methane oxidation since they were identified as presumable syntrophs of ANME-1 archaea in 50°C incubations (Holler *et al.*, 2011). The recovery range of HotSeep-1 phylotypes included the two hottest cores that permitted bacterial DNA recovery, at *in situ* temperatures of 46°C and 49°C (Fig. 5B), suggesting high temperature tolerance, obligate requirements for hydrothermally generated substrates or syntrophic associations within high-temperature ANME consortia (Holler *et al.*, 2011).

Conclusion

Shallow subsurface temperatures can reach extreme levels by just 40 cm depth in Guaymas Basin sediments, limiting microbial colonization to thermally tolerable surface sediments. At *in situ* temperatures above approximately 80°C and 100°C respectively, the ^{13}C-isotopic signatures of microbial anaerobic oxidation and organic matter re-mineralization appear to be thermally restricted and $\delta^{13}C$ values instead reflect those previously reported for methane and DIC in hydrothermal end-member fluids in Guaymas Basin. The isotopic imprint of methane oxidation – leading to ^{13}C enrichment in the residual methane – is visible at *in situ* temperatures below approximately 80°C, while the imprint of organic matter re-mineralization – resulting in ^{13}C-depleted DIC – is only apparent at temperatures below 100°C. Sequence signatures of methane-oxidizing *Archaea* are consistently prominent throughout the predicted thermal range of up to 80°C. While AOM would remain thermodynamically favourable at even higher temperatures, the thermal sensitivity of cells, their enzymes or syntrophic associations most likely determine the actual thermal range of this process. Further, temperature limits must be considered within the framework of the fluctuating hydrothermal regime, which may vary by 25°C in hot sediment layers over the course of a few days, thereby forestalling the development of permanent microbial niches. In this light, the sedimentary habitat conditions at Guaymas Basin would favour not just the development of thermophilic adaptations in *Bacteria* and *Archaea*, but even more so the ability to thrive under strongly fluctuating thermal regimes. We conclude that ANME archaea, in particular, maintain their dominance of the archaeal community at Guaymas Basin by evolutionary diversification in response to hydrothermal conditions and adaptation to fluctuating *in situ* temperatures. In this view, the dynamic hydrothermal conditions of Guaymas Basin constitute an evolutionary laboratory that contributes to the continuing diversification of ANME lineages within the global hydrocarbon seep microbiome (Ruff *et al.*, 2015).

References

Bazylinski, D.A., Farrington, J.W., and Jannasch, H.W. (1988) Hydrocarbons in surface sediments from a Guaymas Basin hydrothermal vent site. *Org Geochem* **12:** 547–558.

Biddle, J.F., Cardman, Z., Mendlovitz, H., Albert, D.B., Lloyd, K.G., Boetius, A., and Teske, A. (2012) Anaerobic oxidation of methane at different temperature regimes in Guaymas Basin hydrothermal sediments. *ISME J* **6:** 1018–1031.

DeLong, E.F. (1992) Archaea in coastal marine environments. *Proc Natl Acad Sci USA* **89:** 5685–5689.

Dhillon, A., Teske, A., Dillon, J., Stahl, D.A., and Sogin, M.L. (2003) Molecular characterization of sulfate-reducing bacteria in the Guaymas Basin. *Appl Environ Microbiol* **69:** 2765–2772.

Didyk, B.M., and Simoneit, B.R.T. (1989) Hydrothermal oil of Guaymas Basin and implications for petroleum formation mechanisms. *Nature* **342:** 65–69.

Dojka, M.A., Hugenholtz, P., Haack, S.K., and Pace, N.R. (1998) Microbial diversity in a hydrocarbon- and chlorinated-solvent-contaminated aquifer undergoing intrinsic bioremediation. *Appl Environ Microbiol* **64:** 3869–3877.

Einsele, G., Gieskes, J.M., Curray, J., Moore, D.M., Aguayo, E., Aubry, M.-P., *et al.* (1980) Intrusion of basaltic sills into highly porous sediments, and resulting hydrothermal activity. *Nature* **283:** 441–445.

Elsgaard, L., Isaksen, M.F., Jørgensen, B.B., Alayse, A.M., and Jannasch, H.W. (1994) Microbial sulfate reduction in deep-sea sediments at the Guaymas Basin hydrothermal vent area: influence of temperature and substrates. *Geochim Cosmochim Acta* **58:** 3335–3343.

Gundersen, J.K., Jørgensen, B.B., Larsen, E., and Jannasch, H.W. (1992) Mats of giant sulphur bacteria on deep-sea sediments due to fluctuating hydrothermal flow. *Nature* **360:** 454–456.

Head, I.M., Jones, M.D., and Larter, S.R. (2003) Biological activity in the deep subsurface and the origin of heavy oil. *Nature* **426:** 344–352.

Hinrichs, K.-U., Hayes, J.M., Sylva, S.P., Brewer, P.G., and DeLong, E.F. (1999) Methane-consuming archaebacteria in marine sediments. *Nature* **398:** 802–805.

Holler, T., Widdel, F., Knittel, K., Amann, R., Kellermann, M.Y., Hinrichs, K.-U., *et al.* (2011) Thermophilic anaerobic oxidation of methane by marine microbial consortia. *ISME J* **5:** 1946–1956.

Inagaki, F., Suzuki, M., Takai, K., Oida, H., Sakamoto, T., Aoki, K., *et al.* (2003) Microbial communities associated with geological horizons in coastal subseafloor sediments from the Sea of Okhotsk. *Appl Environ Microbiol* **69:** 7224–7235.

Jørgensen, B.B., Zawacki, L.X., and Jannasch, H.W. (1990) Thermophilic bacterial sulfate reduction in deep-sea sediments at the Guaymas Basin hydrothermal vents (Gulf of California). *Deep Sea Res I* **37:** 695–710.

Jørgensen, B.B., Isaksen, M.F., and Jannasch, H.W. (1992) Bacterial sulfate reduction above 100°C in deep-sea hydrothermal vent systems. *Science* **258:** 1756–1757.

Kallmeyer, J., and Boetius, A. (2004) Effects of temperature and pressure on sulfate reduction and anaerobic oxidation of methane in hydrothermal sediments of Guaymas Basin. *Appl Environ Microbiol* **70:** 1231–1233.

Kellermann, M.Y., Wegener, G., Elvert, M., Yoshinaga, M.Y., Lin, Y.-S., Holler, T., *et al.* (2012) Autotrophy as a predominant mode of carbon fixation in anaerobic methane-oxidizing microbial communities. *Proc Natl Acad Sci USA* **109:** 19321–19326.

Kelley, D.S., Karson, J.A., Gretchen, L.F.-G., Yoerger, D.R., Shank, T.M., Butterfield, D.A., *et al.* (2005) A serpentinite-hosted ecosystem: the lost city hydrothermal field. *Science* **307:** 1428–1434.

Kniemeyer, O., Musat, F., Sievert, S.M., Knittel, K., Wilkes, H., Blumenberg, M., *et al.* (2007) Anaerobic oxidation of short-chain hydrocarbons by marine sulphate-reducing bacteria. *Nature* **449:** 898–901.

Knittel, K., and Boetius, A. (2009) Anaerobic oxidation of methane: progress with an unknown process. *Annu Rev Microbiol* **63:** 311–334.

LaRowe, D.E., Dale, A.W., and Regnier, P. (2008) A thermodynamic analysis of the anaerobic oxidation of methane in marine sediments. *Geobiol* **6:** 436–449.

LaRowe, D.E., Dale, A.W., Aguilera, D.R., L'Heureux, I., Amend, J.P., and Regnier, P. (2014) Modeling microbial reaction rates in a submarine hydrothermal vent chimney wall. *Geochim Cosmochim Acta* **124:** 72–97.

Lizarralde, D., Axen, G.J., Brown, H.E., Fletcher, J.M., González-Fernández, A., Harding, A.J., *et al.* (2007) Variation in styles of rifting in the Gulf of California. *Nature* **448:** 466–469.

McKay, L.J., MacGregor, B.J., Biddle, J.F., Albert, D.B., Mendlovitz, H.P., Hoer, D.R., *et al.* (2012) Spatial heterogeneity and underlying geochemistry of phylogenetically diverse orange and white *Beggiatoa* mats in Guaymas Basin hydrothermal sediments. *Deep-Sea Res I* **67:** 21–31.

Merkel, A.Y., Huber, J.A., Chernyh, N.A., Bonch-Osmolovskaya, E.A., and Lebedinsky, A.V. (2013) Detection of a putatively thermophilic anaerobic methanotrophs in diffuse hydrothermal vent fluids. *Appl Environ Microbiol* **79:** 915–923.

Meyer, S., Wegener, G., Lloyd, K.G., Teske, A., Boetius, A., and Ramette, A. (2013) Microbial habitat connectivity across spatial scales and hydrothermal temperature gradients at Guaymas Basin. *Front Microbiol* **4:** 207. doi:10.3389/fmicb.2013.00207.

Milucka, J., Ferdelman, T.G., Polerecky, L., Franzke, D., Wegener, G., Schmid, M., *et al.* (2012) Zero-valent sulphur is a key intermediate in marine methane oxidation. *Nature* **491:** 541–546.

Muyzer, G., and Stams, A.J.M. (2008) The ecology and biotechnology of sulphate-reducing bacteria. *Nat Rev Microbiol* **6:** 441–454.

Orphan, V.J., Hinrichs, K.-U., Paull, C.K., Taylor, L.T., Sylva, S., and Delong, E.F. (2001) Comparative analysis of methane-oxidizing archaea and sulfate-reducing bacteria in anoxic marine sediments. *Appl Environ Microbiol* **67:** 1922–1934.

Pearson, A., Seewald, J.S., and Eglinton, T.I. (2005) Bacterial incorporation of relict carbon in the hydrothermal environment of Guaymas Basin. *Geochim Cosmochim Acta* **69:** 5477–5486.

Ruff, E., Biddle, J.F., Teske, A.P., Knittel, K., Boetius, A., and Ramette, A. (2015) Global dispersion and local diversification of the methane seep microbiome. *Proc Natl Acad Sci USA* doi:10.1073/pnas.1421865112.

Schouten, S., Wakeham, S.G., Hopmans, E.C., and Sinninghe Damsté, J.S. (2003) Biogeochemical evidence that thermophilic *Archaea* mediate the anaerobic oxidation of methane. *Appl Environ Microbiol* **69:** 1680–1686.

Seewald, J.S., Cruse, A.M., Lilley, M.D., and Olson, E.J. (1998) Hot-spring fluid chemistry at Guaymas Basin, Gulf of California: temporal variations and volatile content. *Eos (Washington DC)* **79:** 46.

Takai, K., and Horikoshi, K. (1999) Genetic diversity of *Archaea* in deep-sea hydrothermal vent environments. *Genetics* **152:** 1284–1297.

Takai, K., Nakamura, K., Toki, T., Tsunogai, U., Miyazaki, M., Miyazaki, J., *et al.* (2008) Cell proliferation at 122°C and isotopically heavy CH_4 production by a hyperthermophilic methanogen under high-pressure cultivation. *Proc Natl Acad Sci USA* **105:** 10949–10954.

Teske, A., Hinrichs, K.-U., Edgcomb, V., de Vera Gomez, A., Kysela, D., Sylva, S.P., *et al.* (2002) Microbial diversity in hydrothermal sediments in the Guaymas Basin: evidence for anaerobic methanotrophic communities. *Appl Environ Microbiol* **68:** 1994–2007.

Teske, A., Callaghan, A.V., and LaRowe, D.E. (2014) Biosphere frontiers of subsurface life in the sedimented hydrothermal system of Guaymas Basin. *Front Microbiol* **5:** 362. doi:10.3389/fmicb.2014.00362.

Tijhuis, L., van Loosdrecht, M.C.M., and Heijnen, J.J. (1993) A thermodynamically balanced correlation for maintenance Gibbs energy requirements in aerobic and anaerobic chemotrophic growth. *Biotechnology and Bioengineering* **42:** 509–519.

Tsunogai, U., Yoshida, N., Ishibashi, J., and Gamo, T. (2000) Carbon isotopic distribution of methane in deep-sea hydrothermal plume, Myojin Knoll Caldera, Izu-Bonin arc: implications for microbial methane oxidation in the oceans and applications to heat flux estimation. *Geochim Cosmochim Acta* **64:** 2439–2452.

Vetriani, C., Jannasch, H.W., MacGregor, B.J., Stahl, D.A., and Reysenbach, A.L. (1999) Population structure and

phylogenetic characterization of marine benthic archaea in deep-sea sediments. *Appl Environ Microbiol* **65:** 4375–4384.

Von Damm, K.L., Edmond, J.M., Measures, C.I., and Grant, B. (1985) Chemistry of submarine hydrothermal solutions at Guaymas Basin, Gulf of California. *Geochim Cosmochim Acta* **49:** 2221–2237.

Weber, A., and Jørgensen, B.B. (2002) Bacterial sulfate reduction in hydrothermal sediments of the Guaymas Basin, Gulf of California, Mexico. *Deep Sea Res I* **49:** 827–841.

Webster, G., Parkes, R.J., Fry, J.C., and Weightman, A.J. (2004) Widespread occurrence of a novel division of bacteria identified by 16S rRNA gene sequences originally found in deep marine sediments. *Appl Environ Microbiol* **70:** 5708–5713.

Welhan, J.A., and Craig, H. (1983) Methane, hydrogen and helium in hydrothermal fluids of 21°N on the East Pacific Rise. In *Hydrothermal Processes at Seafloor Spreading Centers*. Rona, P.A. *et al.* (eds.). New York, NY, USA: Plenum, pp. 391–409.

Welhan, J.A., and Lupton, J.E. (1987) Light hydrocarbon gases in Guaymas Basin hydrothermal fluids: thermogenic versus abiogenic origin. *AAPB Bull* **71:** 215–223.

Welhan, L.A. (1988) Origins of methane in hydrothermal systems. *Chem Geol* **71:** 183–1988.

Supporting information

Additional Supporting Information may be found in the online version of this article at the publisher's website:

Fig. S1. Principal components analyses of microbial community composition.

Fig. S2. Complete archaeal (A) and bacterial (B) neighbour-joining 16S rRNA gene phylogeny.

Fig. S3. 16S rRNA gene sequence phylogeny detailing paraphyly of *Deltaproteobacteria*, HotSeep-1 group and the *Hippea* cluster.

Fig. S4. Concentration and stable isotope measurements for methane (A) and DIC (B) with corresponding temperature data.

Table S1. Concentrations and del13C values for methane and DIC from 36 sediment cores retrieved in 2008 and 2009 by the HOV *Alvin* submersible. Corresponding temperatures from adjacent thermal profiles are also presented, with real values in black and interpolated values in red. Interpolations were determined by selecting the best fit line to measured thermal profiles as indicated by the highest achievable r squared value.